PHYSICAL REVIEW A **87**, 042502 (2013)

Thallium 7*p* lifetimes derived from experimental data and *ab initio* calculations of scalar polarizabilities

M. S. Safronova[1,2] and P. K. Majumder[3]
[1]*Department of Physics and Astronomy, University of Delaware, Newark, Delaware 19716, USA*
[2]*Joint Quantum Institute, NIST and the University of Maryland, College Park, Maryland 20742, USA*
[3]*Physics Department, Williams College, Williamstown, Massachusetts 01267, USA*

(Received 7 March 2013; published 3 April 2013)

Two different theoretical methods have been used to complete a calculation of polarizability in the thallium $6p_{1/2}$, $7s$, and $7p_{1/2}$ states. The predictions of the two methods agree to within 1% for the $6p_{1/2}$ and $7s$ states and 2% for the $7p_{1/2}$ state. We find that the theoretical expression for the $6p_{1/2}$-$7s$ transition polarizability difference $\Delta\alpha_0$ is dominated (greater than 90% contribution) by mixing of the $7s$ state with the $7p_{1/2}$ and $7p_{3/2}$ states. By comparing the theoretical expression to an existing measurement of $\Delta\alpha_0$ [Doret *et al.*, Phys. Rev. A **66**, 052504 (2002)], highly accurate values for the thallium $7p$ excited-state lifetimes have been extracted. The scalar polarizability of the $7p_{1/2}$ state is also computed, anticipating an experimental determination of this quantity, which will then enable a high-precision determination of the $6d_j$-$7p_{j'}$ transition rates and provide a benchmark test of the two theoretical approaches in the near future.

DOI: 10.1103/PhysRevA.87.042502 PACS number(s): 32.70.Cs, 32.60.+i, 31.15.ap, 31.15.ac

I. INTRODUCTION

Thallium has played an important role in atomic-physics-based tests of discrete symmetry violation over recent decades [1–3]. The size of these symmetry-violating observables scales rapidly with the atomic number, encouraging the use of high-Z systems. This therefore requires independent, precise atomic wave-function calculations in order to distinguish quantum-mechanical effects from the elementary-particle physics observables being targeted. For example, theoretical uncertainties in *ab initio* wave-function calculations in thallium currently limit the quality of the standard model test provided by a 1995 thallium parity-nonconservation measurement [2,4]. Similarly, high-precision atomic theory is essential to interpret results from searches for atomic and molecular electric dipole moments (EDMs), as evidenced by recent calculations of the thallium EDM enhancement factor [3,5–7]. Independent, high-precision atomic structure measurements serve as an important tool in testing the accuracy and guiding the refinement of theoretical techniques for multielectron systems such as thallium. Over recent years, we have completed precise measurements of thallium transition amplitudes [8], hyperfine splittings [9], and polarizability [10] which show excellent agreement with theory [11,12]. More recently, a similar theoretical approach to that used for thallium has also been applied to other trivalent group IIIA systems such as indium and gallium [13,14].

Very recently, theoretical work and experimental work have come together in the indium atomic system. A measurement of the Stark shift within the indium 410-nm $5p_{1/2}$-$6s_{1/2}$ transition [15] yielded a value for the $6s$-$5p_{1/2}$ polarizability difference with 0.3% uncertainty. At the same time, a new *ab initio* theory effort, using two complementary, high-precision techniques, yielded a theoretical value for this quantity in excellent agreement with the experimental result and with 2% estimated uncertainty [14]. Because the theoretical expression for the $6s$ polarizability is dominated by terms involving the $6s$-$6p_{1/2}$ and $6s$-$6p_{3/2}$ mixing, we show in Refs. [14,15] that a comparison of experimental and theoretical results can produce new values for the $6p$-state lifetimes with uncertainties below 1%.

In this paper, a similar approach of combining high-precision calculation and experiment is applied to thallium. An extensive calculation including uncertainties is undertaken using both a coupled-cluster (CC) approach as well as a configuration interaction + all-order (CI + all-order) approach to compute the polarizability of the thallium $6p_{1/2}$ ground state, as well as the $7s$ and $7p_{1/2}$ excited states. We use a comparison of this theory to the 2002 thallium Stark shift result [10] to extract the most precise values to date for the thallium $7p$-state lifetimes. We also outline ongoing experimental work which will allow precise measurements of excited-state Stark shifts in both thallium and indium. Such measurements will then be combined with theoretical polarizability results to accurately predict the thallium $6d$-$7p$ and indium $5d$-$6p$ transition rates.

II. CALCULATION OF POLARIZABILITIES

The valence static polarizabilities of a Tl atom can be calculated as a sum over states:

$$\alpha_0 = \frac{2}{3(2J+1)} \sum_n \frac{|\langle J||D||J_n\rangle|^2}{E_n - E}, \tag{1}$$

where the sum over n runs over all states with allowed $\langle J||D||J_n\rangle$ electric dipole transitions. The $7s$-$6p_{1/2}$ Stark shift in Tl (i.e., the difference of the $7s$ and $6p_{1/2}$ polarizabilities) is strongly dominated by the contributions from the $7s$-$7p_j$ transitions to the $7s$ polarizability. Therefore, accurate measurement of this Stark shift carried out in [10] can be used to extract $7s$-$7p_j$ matrix elements if all other smaller contributions to the $6p_{1/2}$ and $7s$ polarizabilities are calculated. The extraction of the matrix elements also require the evaluation of relevant theoretical uncertainties. Combining $7s$-$7p_j$ matrix elements with experimental transition energies [16] gives the $7p_{1/2}$ and $7p_{3/2}$ lifetimes.

The polarizabilities of the ground $6p_{1/2}$ and excited $7s$ states were calculated using the linearized coupled-cluster method in [12], but their uncertainties were not evaluated. In this work, we carry out additional linearized coupled-cluster calculations (CC) to estimate the uncertainties of each term. We also carry out another independent calculation of these polarizabilities using a recently developed hybrid approach that combines configuration interaction and the linearized coupled-cluster method (CI + all-order) [19]. This calculation treats Tl as a system with three valence electrons and accurately accounts for configuration mixing and valence-valence correlations. The CC calculation treats Tl as a monovalent system with $6s^2$ considered to be a part of the closed core; however, the CC approach includes some additional high-order corrections to the dipole operator. Since these two methods differ in their inclusion of higher-order effects, comparing their results provides additional evaluation of the uncertainty of our calculations. We refer the reader to Refs. [12,20,21] and [3,19,22–25] for detailed descriptions of the linearized coupled-cluster and CI + all-order methods, respectively. The results of both methods were recently compared for In polarizabilities in [14].

The breakdown of the contributions to the $7s$ and $6p_{1/2}$ Tl polarizabilities is listed in Table I. Experimental energies are given for all terms that are listed separately, such as $7p$ contributions to the $7s$ polarizability. The uncertainties of the main CC terms are determined from the spread of four different coupled-cluster calculations carried out in this work (with and without the perturbative triple terms and with inclusion of the scaling to account for some missing higher-order corrections); CC matrix elements from [12] are kept as final values. The determination of the uncertainties is described in detail in Refs. [14,21]. The $(n > 8)$ contributions for the $7s$ polarizability contain the $9p$ contribution calculated using the all-order method and all other $(n > 9)$ terms calculated in the random-phase approximation (RPA) and scaled to account for higher-order corrections. The scaling factor is determined as the ratio of the total CC value for the main $n = 6$–9 terms and corresponding RPA result. For the $6p_{1/2}$ polarizability, $(7$–$10)s$ and $(6$–$9)d_{3/2}$ contributions are calculated by combining CC matrix elements and experimental energies, and the remaining contributions are calculated together using the scaled RPA approach. The difference of the *ab initio* RPA and scaled RPA values is taken to be the uncertainty of these high-n contributions. The ionic core polarizabilities and small (vc) term that accounts for the occupied valence shell(s) are listed separately in the core and vc rows. The vc term is negligible for the $7s$ and $7p_{1/2}$ polarizabilities. Core and vc contributions are calculated in the RPA. The differences of the Dirac-Fock and RPA values are taken to be their uncertainties. We note that core polarizability is much larger in the CC method since the $6s^2$ shell is included in the core in the CC calculation, while the $6s$ shell belongs to the valence space in the trivalent CI + all-order calculation.

The sum over states is not used in the CI + all-order calculation of the polarizabilities, which is carried out by solving the inhomogeneous equation of perturbation theory in the valence space [26]. However, we evaluated a few dominant terms separately by combining CI + all-order matrix elements with experimental energies to compare these terms in both approaches. These results are listed in the last column of Table I.

TABLE I. Contributions to the $7s$, $6p_{1/2}$, and $7p_{1/2}$ static polarizabilities are given in units of a_0^3 in columns labeled α_0. The experimental energies [16] (in cm^{-1}) and the theoretical electric-dipole reduced matrix elements (in a.u.) used to calculate dominant contributions are listed in columns labeled ΔE and D. The CC and CI + all-order electric-dipole matrix elements and the polarizability contributions are listed in columns labeled CC and CI + All, respectively.

	ΔE	D		α_0	
Contribution	Expt.	CC	CI + All	CC	CI + All
		$7s$ polarizability			
$6p_{1/2}$	−26478	1.826	1.798	−9.2(4)	−8.9
$7p_{1/2}$	7682	6.016	6.050	345(12)	349
$8p_{1/2}$	14891	0.706	0.693	2.4(5)	2.4
$(n > 8)p_{1/2}$				0.7(2)	
$6p_{3/2}$	−18685	3.397	3.395	−45(2)	−45
$7p_{3/2}$	8684	8.063	8.108	548(22)	554
$8p_{3/2}$	15263	1.474	1.509	10(1)	11
$(n > 8)p_{3/2}$				5(1)	
Core				24(1)	5
Total				881(25)	887
		$6p_{1/2}$ polarizability			
$7s$	26478	1.826	1.798	9.2(5)	8.9
$8s$	38746	0.535		0.54(5)	
$(n > 8)s$				0.8(3)	
$6d_{3/2}$	36118	2.334	2.377	11.0(4)	11.5
$7d_{3/2}$	42011	1.101		2.1(1)	
$(n > 8)d_{3/2}$				6.4(2.8)	
Core				24.1(1.2)	5.0
vc				−4.2(9)	−0.4
Total				50.0(3.0)	50.7
		$7p_{1/2}$ polarizability			
$7s$	−7682	6.013	6.050	−344(3)	−349
$8s$	4586	6.189		611(5)	
$(n > 8)s$				22(1)	
$6d_{3/2}$	1958	10.726	10.649	4298(24)	4237
$7d_{3/2}$	7852	4.767		212(13)	
$(n > 8)d_{3/2}$				95(13)	
Core				24(1)	5
Total				4918(30)	4831
Final				4918(120)	

We also calculated the thallium $7p_{1/2}$ polarizability using both CC and CI + all-order methods. Since the $7p_{1/2}$-$6d_{3/2}$ matrix element strongly dominates $7p_{1/2}$ polarizability, our calculation can be used to extract this matrix element if either the $7p_{1/2}$-$6p_{1/2}$ or $7p_{1/2}$-$7s$ Stark shift is measured with high precision. We have used the $7s$-$7p_{1/2}$ matrix element determined in the next section to provide a more accurate recommended value. We determine the contribution of all other terms except the $7p_{1/2}$-$6d_{3/2}$ term to be 620(36) a.u. (see Table I). The determination of the final uncertainties is described in the next section.

III. DETERMINATION OF THALLIUM 7*p* LIFETIMES

Separating the $7s$-$7p_j$ contributions [see Eq. (1)], we write the $\Delta\alpha_0(7s - 6p_{1/2})$ Stark shift as

$$\Delta\alpha_0(7s - 6p_{1/2}) = BS + C, \tag{2}$$

TABLE II. Final values of the $7s$ and $6p_{1/2}$ polarizabilities and their difference $\Delta\alpha_0$ (a.u.). Determination of the reduced electric-dipole $7s$-$7p_j$ matrix elements (in a.u.) and $7p_j$ lifetimes (in ns) from the combination of measured Stark shift [10] and theoretical values. The quantity C is the value of $\Delta\alpha_0(7s-6p_{1/2})$ with the contribution of the $7s$-$7p_j$ transitions subtracted out.

	$\alpha_0(7s)$	$\alpha_0(6p_{1/2})$	$\Delta\alpha_0(7s-6p_{1/2})$	C	$D(7s-7p_{1/2})$	$D(7s-7p_{3/2})$	$\tau(7p_{1/2})$	$\tau(7p_{3/2})$
CC	881	50.0	831	−61.7	6.016	8.063	60.15	46.38
CI + All	887	50.7	836	−66.4	6.050	8.108	59.48	45.86
Final	881(9)	50.0(1.0)	831(8)	−61.7(6.7)	6.013(27)	8.058(37)	60.21(55)	46.44(42)
Expt.		51(7)[a]	829.7(3.1)[b]					
Theory		49.2,[c] 48.8[d]						
Theory		52.1(1.6)[e]						

[a] Reference [17].
[b] Reference [10].
[c] Reference [4].
[d] Reference [6].
[e] Reference [18].

where

$$B = \frac{1}{3}\left(\frac{1}{E(7p_{1/2})-E(7s)} + \frac{R^2}{E(7p_{3/2})-E(7s)}\right), \qquad (3)$$

$S = D^2$ is the $7s$-$7p_{1/2}$ line strength, R is the ratio of the $D(7s-7p_{3/2})$ and $D(7s-7p_{1/2})$ reduced $E1$ matrix elements $R = 1.340(4)$, and term C contains all other contributions to the Stark shift. We use the $\Delta\alpha_0(7s-6p_{1/2})$ measured in Ref. [10]. Combining experimental energies from [16] and our theoretical value of the ratio gives $B = 24.65(9)$ a.u. The final results of our calculations for $6p_{1/2}$ and $7s$ polarizabilities, their difference, and term C are given in Table II. Our theoretical value for the $7s$-$6p_{1/2}$ Stark shift is in excellent agreement with the experiment [10]. The ground-state polarizability is compared with theory [4,6,18] and experiment [17]. Since CC and CI + all-order values include all dominant correlation corrections between these two calculations, we estimate the uncertainty in the dominant contributions as the difference between the CC and CI + all-order values $\delta\alpha$. Then, we assume that all other uncertainties do not exceed the uncertainty of the dominant corrections $\delta\alpha$. Adding these uncertainties in quadrature, we arrive at the total uncertainty of $\sqrt{2}\delta\alpha$. The uncertainty in term C is determined by the same procedure. The uncertainty in the $7s$-$7p_{1/2}$ line strength S is determined as

$$\delta S = \frac{1}{B}\sqrt{(\delta C)^2 + (\delta\Delta\alpha_0)^2 + (S\delta B)^2}. \qquad (4)$$

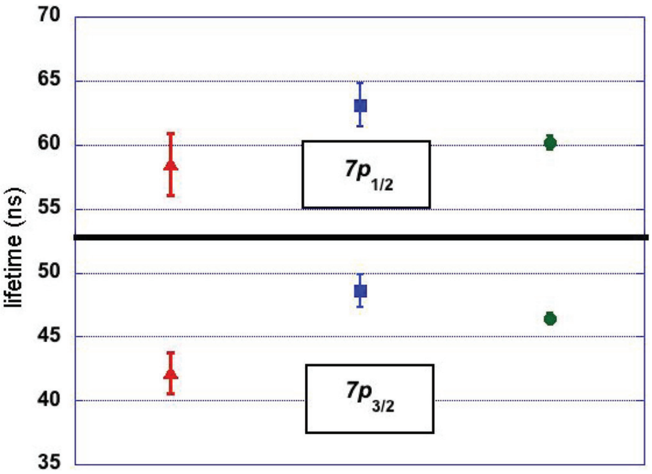

FIG. 1. (Color online) A comparison of the present $7p$-state lifetime determinations to older experimental results. (top) The $7p_{1/2}$ results and (bottom) the $7p_{3/2}$ results. References are as follows: red triangles, Ref. [27]; blue squares, Ref. [28]; green circles, present work.

The lifetimes of the $7p_j$ states are obtained using $\tau_a = 1/A_{ab}$, where the transition rate A_{ab} is given by

$$A_{ab} = \frac{2.02613\times10^{18}}{\lambda_{ab}^3}\frac{S_{ab}}{2J_a+1}\ \mathrm{s}^{-1}; \qquad (5)$$

the transition wavelength λ_{ab} is in angstroms. The final recommended values for the $7p_{1/2}$ and $7p_{3/2}$ lifetimes are listed in Table II. The purely theoretical lifetime results of the CC calculation are in very good agreement with these recommended values. Figure 1 compares the present results to earlier experimental determinations of these lifetimes.

IV. MEASUREMENT OF EXCITED-STATE STARK SHIFTS IN THALLIUM AND INDIUM

As described here, as well as in [14], calculations of the excited p-state polarizabilities, coupled with future measurements of excited-state Stark shifts, will allow important new tests of the atomic theory. In particular, a measurement of the Stark shifts involving $7p$ states in Tl and the $6p$ state in In will allow a definitive test of the CC and CI + all-order theoretical methods. While both approaches give results in very close agreement for the ground state and the first excited ns state polarizabilities of In and Tl, the differences increase for the next excited np state polarizability (to 2% for Tl and 4% for In [14]). Precise Stark shift measurements involving these excited np states will directly address the question of whether accurate treatment of the configuration mixing or higher-order corrections to the matrix elements are more important for such states. Moreover, measurement of these Stark shifts will allow determination of the $7p$-$6d$ transition rates in Tl and $6p$-$5d$ transition rates in In. These are very important for improved theoretical descriptions of the d-state properties.

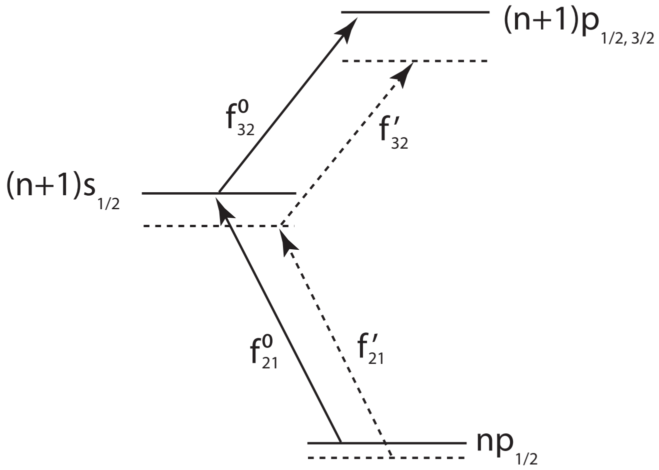

FIG. 2. A schematic diagram showing the configuration of low-lying energy levels of both thallium and indium. The dotted lines suggest the Stark-shifted levels, where the size of the level shifts (not to scale) become successively larger for the higher-lying states.

These rates cannot be determined accurately from *nd*-state lifetime measurements such as reported in [29] owing to very small branching ratios.

We are currently undertaking atomic-beam-based experiments to measure the excited *p*-state polarizabilities in both thallium and indium. To achieve this, having completed Stark shift experiments in the ground-state 410-nm and 378-nm transitions of these two group IIIA elements, we are now introducing a two-step, two-color spectroscopy measurement scheme for use with our atomic-beam apparatus. For both atomic systems, we have completed such two-step spectroscopy experiments in a vapor cell environment to study excited-state hyperfine structure and isotope shifts [30,31]. In these two-step experiments, we begin by locking the blue or UV laser to the first transition step, using a supplementary atomic vapor cell and a technique developed recently [32]. We then overlap this laser beam with that of a second infrared laser and intersect both with our atomic beam using a transverse geometry. Interestingly, the thallium $7s$-$7p_{1/2}$ and the indium $6s$-$6p_{1/2}$ and $6s$-$6p_{3/2}$ transitions, with resonance wavelengths of 1301, 1343, and 1291 nm, respectively, can all be reached by a single external cavity diode laser which is currently in use (Sacher Lasertechnik, model TEC-150-1300-050). Using the FM spectroscopy technique described in [15], we will extract high-resolution spectra from the atomic-beam transmission signal of the infrared laser, expected to be an order of magnitude weaker than the signal from the analogous single-step experiment, given that here we promote only a fraction of the ground-state atoms to the intermediate state.

In general, extracting Stark shift information in a two-step transition experiment is complicated by the fact that both transitions are shifted when the static field is turned on. Figure 2 indicates the general form of such a three-level, two-step process in either indium or thallium. As indicated, in the presence of an electric field, all energy levels are Stark-shifted downwards, with the magnitude of the shift increasing for higher-lying states. We define the magnitude of the Stark shift within the lower (upper) transition as Δ_{21} (Δ_{32}) and the field-free resonance frequency of this transition as f^0_{21} (f^0_{32}). We note that for both elements $\Delta_{32} \gg \Delta_{21}$. By keeping the first-step laser locked to the atomic transition in a *field-free* region, the first-step excitation in the electric field region would then be shifted slightly out of resonance. This results in the excitation of a nonzero velocity class of atoms. In this case, the resonance frequency for the second-step transition, f'_{32}, in the presence of the electric field is given by

$$f'_{32} = f^0_{32} - |\Delta_{32}| + |\Delta_{21}|\frac{f_{32}}{f_{21}}, \tag{6}$$

where the final term results from the Doppler shift produced by the off-resonant first-step excitation. For an electric field of 10 kV/cm, typical for these experiments, $\Delta_{21} \approx 10$ MHz, which is still much less than the ~100 MHz residual Doppler width in the atomic-beam geometry. Thus, the decrease in excitation efficiency for the first-step transition in the presence of the electric field will not be significant. Furthermore, since the optical resonance frequencies f_{21} and f_{32} in Eq. (6) are known and Δ_{21} has been previously measured to high accuracy [10], we will be able to determine Δ_{32} unambiguously. For transitions involving $J = 1/2$ states, there is only a scalar component to the polarizability, but for the indium 1291-nm $6s$-$6p_{3/2}$ transition, there will exist both scalar and tensor contributions, both of which were computed in [14]. In this case we will study each resolved hyperfine transition and will vary the laser polarization relative to the static field direction to extract both polarizability components.

V. CONCLUSIONS

In conclusion, through a comparison of an existing thallium Stark shift measurement and *ab initio* calculations of scalar polarizabilities, we have derived highly accurate values for the thallium $7p$ excited-state lifetimes. Recent measurements of Stark shifts in thallium and indium serve an important function as benchmark tests of two distinct atomic theory techniques that can be applied to these multivalence systems. Future measurements of excited-state Stark shifts in both elements will test the atomic theory approaches in important new ways since the relevant polarizability is dominated by mixing with excited d states in these systems, whose theoretical contributions are more uncertain. A theory-experiment comparison will thus allow precise derivation of thallium $7p$-$6d$ and indium $6p$-$5d$ transition matrix elements.

ACKNOWLEDGMENTS

We thank U. I. Safronova and S. G. Porsev for useful discussions. The work of M.S.S. was supported in part by NSF Grant No. PHY-1068699. We thank G. Ranjit and N. A. Schine for important experimental contributions. The experimental polarizability work was supported by NSF Grant No. PHY-0140189 and is currently supported by Grant No. PHY-0969781.

[1] B. C. Regan, E. D. Commins, C. J. Schmidt, and D. DeMille, Phys. Rev. Lett. **88**, 071805 (2002).

[2] P. A. Vetter, D. M. Meekhof, P. K. Majumder, S. K. Lamoreaux, and E. N. Fortson, Phys. Rev. Lett. **74**, 2658 (1995).

[3] S. G. Porsev, M. S. Safronova, and M. G. Kozlov, Phys. Rev. Lett. **108**, 173001 (2012).

[4] M. G. Kozlov, S. G. Porsev, and W. R. Johnson, Phys. Rev. A **64**, 052107 (2001).

[5] H. S. Nataraj, B. K. Sahoo, B. P. Das, and D. Mukherjee, Phys. Rev. Lett. **106**, 200403 (2011).

[6] V. A. Dzuba and V. V. Flambaum, Phys. Rev. A **80**, 062509 (2009).

[7] Z. W. Liu and H. P. Kelly, Phys. Rev. A **45**, R4210 (1992).

[8] P. K. Majumder and L. L. Tsai, Phys. Rev. A **60**, 267 (1999).

[9] D. S. Richardson, R. N. Lyman, and P. K. Majumder, Phys. Rev. A **62**, 012510 (2000).

[10] S. C. Doret, P. D. Friedberg, A. J. Speck, D. S. Richardson, and P. K. Majumder, Phys. Rev. A **66**, 052504 (2002).

[11] U. I. Safronova, M. S. Safronova, and W. R. Johnson, Phys. Rev. A **71**, 052506 (2005).

[12] M. S. Safronova, W. R. Johnson, U. I. Safronova, and T. E. Cowan, Phys. Rev. A **74**, 022504 (2006).

[13] U. I. Safronova, M. S. Safronova, and M. G. Kozlov, Phys. Rev. A **76**, 022501 (2007).

[14] M. S. Safronova, U. I. Safronova, and S. G. Porsev, Phys. Rev. A **87**, 032513 (2013).

[15] G. Ranjit, N. A. Schine, A. T. Lorenzo, A. E. Schneider, and P. K. Majumder, Phys. Rev. A **87**, 032506 (2013).

[16] Yu. Ralchenko, A. Kramida, J. Reader, and NIST ASD Team, NIST Atomic Spectra Database (version 4.1), http://physics.nist.gov/asd

[17] *CRC Handbook of Chemistry and Physics*, 93rd ed., edited by W. M. Haynes (Internet Version 2013) (CRC Press/Taylor and Francis, Boca Raton, FL, 2013), pp. 10–189.

[18] A. Borschevsky, T. Zelovich, E. Eliav, and U. Kaldor, Chem. Phys. **395**, 104 (2012).

[19] M. S. Safronova, M. G. Kozlov, W. R. Johnson, and D. Jiang, Phys. Rev. A **80**, 012516 (2009).

[20] M. S. Safronova and W. R. Johnson, Adv. At. Mol. Opt. Phys. **55**, 191 (2008).

[21] M. S. Safronova and U. I. Safronova, Phys. Rev. A **83**, 052508 (2011).

[22] M. S. Safronova, S. G. Porsev, and C. W. Clark, Phys. Rev. Lett. **109**, 230802 (2012).

[23] M. S. Safronova, M. G. Kozlov, and C. W. Clark, Phys. Rev. Lett. **107**, 143006 (2011).

[24] M. S. Safronova, M. G. Kozlov, and U. I. Safronova, Phys. Rev. A **85**, 012507 (2012).

[25] M. S. Safronova, S. G. Porsev, M. G. Kozlov, and C. W. Clark, Phys. Rev. A **85**, 052506 (2012).

[26] S. G. Porsev, Yu. G. Rakhlina, and M. G. Kozlov, Phys. Rev. A **60**, 2781 (1999).

[27] L. Hunter, E. Commins, and L. Roesch, Phys. Rev. A **25**, 885 (1982).

[28] J. V. James, C. C. Wang, and C. Doty, Phys. Rev. A **34**, 1117 (1986).

[29] N. Taylor, N. Omenetto, B. Smith, and J. Winefordner, Appl. Spectrosc. **62**, 78 (2008).

[30] M. Gunawardena, H. Cao, P. W. Hess, and P. K. Majumder, Phys. Rev. A **80**, 032519 (2009).

[31] G. Ranjit, D. Kealhofer, and P. Majumder (to be published).

[32] M. Gunawardena, P. W. Hess, J. Strait, and P. K. Majumder, Rev. Sci. Instrum. **79**, 103110 (2008).